CRYSTAL GROWTH & DESIGN

Article

pubs.acs.org/crystal

Crystallization of $CaCO_3$ in Water–Alcohol Mixtures: Spherulitic Growth, Polymorph Stabilization, and Morphology Change

K. K. Sand,*[,†] J. D. Rodriguez-Blanco,[‡] E. Makovicky,[#] L. G. Benning,[‡] and S. L. S. Stipp[†]

[†]Nano-Science Center, Department of Chemistry, University of Copenhagen, Denmark

[‡]School of Earth and Environment, University of Leeds, United Kingdom

[#]Department of Geography and Geology, University of Copenhagen, Denmark

Supporting Information

ABSTRACT: The presence of alcohol in binary alcohol–water mixtures can affect the precipitation pathways of anhydrous crystalline $CaCO_3$ polymorphs and their morphology. We explored the formation pathways and the effects of several parameters on calcite, vaterite, and aragonite: concentration of simple alcohols, time, and shaking speed, and we derived a multiparameter model for predicting what phase is preferred. We found that shaking speed and alcohol concentration are the most important parameters for affecting the stability of vaterite and aragonite and for changing vaterite morphology, from cauliflower-shaped, spherical aggregates, to dendritic, flatter structures. In all our experiments, the precipitated aragonite was twinned, and both the vaterite and aragonite can be interpreted to form through spherulitic growth. Classical growth theory fully describes their formation; there is no need to invoke the popular hypothesis for nonclassical growth by self-assembly of nanocrystals. These studies, and future work with solutions of low water activity, are paving the way to a better understanding of how organisms select their preferred polymorph and engineer $CaCO_3$ morphology during biomineralization.

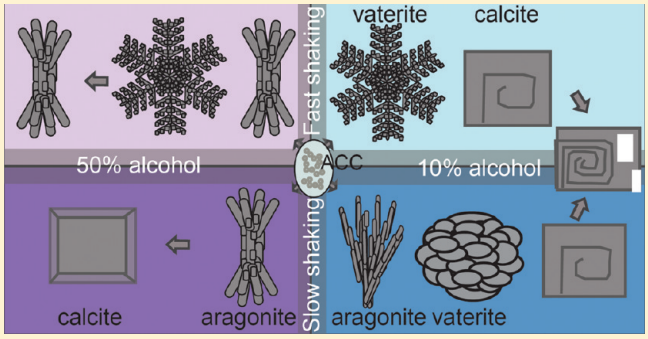

INTRODUCTION

The ability to control calcium carbonate ($CaCO_3$) polymorph stabilization and morphology is necessary for organisms during biomineralization, and it is also important for industrial $CaCO_3$ production, where engineering particle shape and the proportion of polymorphs in mixtures determines the product's end use. $CaCO_3$ has three anhydrous crystalline polymorphs: hexagonal vaterite, orthorhombic aragonite, and rhombohedral calcite. In the pure system, vaterite usually forms polycrystalline spheres, aragonite forms needles, and calcite forms equant rhombs. During homogeneous precipitation at ambient conditions and high saturation index (SI), the first precipitating phase is amorphous calcium carbonate (ACC), which is a hydrous form of $CaCO_3$.[1] The bulk of this phase is generally thermodynamically unstable at ambient conditions. In solution, it usually transforms to vaterite within minutes.[2,3] As the SI drops, vaterite transforms to the most stable polymorph, calcite[4] at temperatures < 40 °C or to aragonite, if T > 40 °C).[2,5] Although ACC and vaterite are thermodynamically unstable, they are commonly found as biominerals; for example, ACC is found in nacre in *Haliotis laevigata* where it covers aragonite platelets,[6] and vaterite exists as spicules in *Ascidiacea*.[7] Calcite exists in intricate morphologies in a great variety of organisms, for example, the elaborate calcite platelets called coccoliths that are formed by some species of algae. An understanding of the mechanisms of polymorph stabilization during biomineralization is interesting academically and for industrial applications.

Several approaches have been taken to address polymorph stabilization and to mimic the elaborate morphologies of $CaCO_3$ biomaterials, for example, by using templates and additives or by choosing appropriate precipitating conditions.[8−12] The process of biomineralization takes place at the interface in a three-phase system, between solid, water, and organic molecules and mineralization generally starts with secretion of an organic template by living cells.[13,14] The exact composition of the cellular fluids and the activity of water at the mineralizing interface are not known, but the activity of water is most likely not unity. Investigations of the effect of changes in solvent properties on $CaCO_3$ precipitation in water–alcohol solutions have shown potential for polymorph discrimination and stability, for example,[8,15−17] but so far, a systematic evaluation of the best way to stabilize specific polymorphs or to design processes to produce specific morphologies is still lacking.

It is generally agreed that alcohol can stabilize the intermediate polymorph vaterite in mixed water–ethanol solutions[16,17] and that alcohol has an influence on vaterite

Received: September 20, 2011
Revised: November 22, 2011
Published: November 29, 2011

   dx.doi.org/10.1021/cg2012342 | *Cryst. Growth Des.* 2012, 12, 842–853

morphology.[16,18] Aragonite has been shown to precipitate at ambient conditions when alcohol is present in the solution,[15,17] and a polymorph discrimination of $CaCO_3$ has been realized by varying the water−ethanol ratio, for example.[8,15,19] The results from research on the effects of alcohols on $CaCO_3$ formation are difficult to combine or compare. The polymorph that dominates has been shown to depend on the time elapsed, precipitation method, the calcium source, and stirring speed.[8] Alcohol has been proposed to have both a chemical and a physical effect on the solution. Chen et al.[8] reported that ethanol has a chemical effect on the solvent, observed as an increase in the SI upon addition. A physical effect is also reported as an incomplete mixing between water and alcohol (ethanol or methanol) molecules.[20−25] We are using the term "stabilization" to mean that the proportion of the "more stable" polymorph increases with time under the given set of experimental conditions.

The mechanisms of formation of the $CaCO_3$ polymorphs with and without additives are discussed extensively in the literature.[9,26−29] Two mechanisms are proposed: classical and nonclassical crystal growth. Classical theory describes ion-by-ion or single molecule attachment to a critical crystal nucleus, with growth by unit cell replication without structural changes in the bulk or at the surface. Nonclassical theory describes a nanoparticle mediated process where primary nanoparticles associate after nucleation by mesoscale assembly into an iso-oriented crystal or, if polymers or other additives are present, transforming into what is termed a mesocrystal.[30] If aggregated nanoparticles are not oriented, the product is called a polycrystal.[29]

In this paper, we exploit the sensitivity of $CaCO_3$ precipitation to various chemical and physical experimental parameters previously reported to be important in the $CaCO_3$−water−alcohol system. We aimed to establish a base for comparison between precipitation outcomes that can easily be applied and modified when the aim is to produce a specific product. Our main purpose was to identify some of the key parameters that influence the precipitation outcome as a function of time. Some of the questions we aimed to answer include: Does the position of the −OH group on the alcohol have a significant influence? Are the physical changes in the solvent important, such that a change in shaking speed can change the precipitation outcome? How much alcohol is needed in each regime to modify the vaterite morphology or to stabilize aragonite? The morphology investigations of the precipitates also allowed us to address the growth mechanisms qualitatively. Our results can be used to constrain a set of experimental conditions for synthesizing a certain polymorph ratio for calcite/vaterite/aragonite or a particular morphology.

METHODS

We chose a simple precipitation method, where we fixed temperature (24 °C) and the concentration of $CaCl_2$ and Na_2CO_3 (25 mM) and varied the volume proportion (10 and 50%) of added alcohol, shaking speed (gentle versus vigorous), type of simple alcohol (ethanol, 1-propanol and 2-propanol), and reaction time (1 h to 4 months). This approach allowed us to address which parameter or which combination of parameters were the most effective for polymorph discrimination and the cause of morphology change.

All starting materials were of analytic reagent grade: calcium chloride ($CaCl_2$; Sigma-Aldrich) and sodium carbonate (Na_2CO_3; Merck KGaA). We used ultrapure deionized (DI) water (Milli-Q; resistivity >18 MΩ cm^{-1}; Millipore Corporation). The ethanol was purchased from Lab Scan, 1-propanol from Sigma Aldrich, and 2-propanol from Fluka. The alcohols were HPLC or reagent grade. All chemicals were used as purchased.

For the synthesis of the calcium carbonate with 10 and 50 volume percent alcohol, stock solutions of Na_2CO_3 and $CaCl_2$ in DI were prepared. In the total reaction volume of 1 L, the final concentration of the Na_2CO_3 and $CaCl_2$ was 25 mM, if the alcohols are considered as part of the liquid. We used a large reaction volume because we only allowed a maximum of 10% decrease in the reaction volume resulting from sequential sampling, to avoid a risk of changing the reaction pathway. In a typical synthesis, 10 or 50 volume percent alcohol (ethanol, 1-propanol, or 2-propanol) was added to a 1 L SIMAX glass bottle. The Na_2CO_3 was added to the alcohol and shaken vigorously for 5 s to ensure mixing. The $CaCl_2$ was added to the mixture, and the closed bottles were gently turned upside down five times before being placed on a shaking board.

For the gently shaken experiments (GS), the shaking board ran at 80 circular revolutions per minute (RPM) with radial shaking movements with an eccentricity of 1.5 cm. For the vigorously shaken experiments (VS), we used 140 rpm at the same eccentricity. The experiments were sampled by removing 20 mL aliquots using a pipet after 1 h, 5 h, 1 day, 1 week, 1 month and 3 months or 4 months. The collected solution was vacuum filtered using cyclopore track etched membranes with a pore size of 0.4 μm. After filtration, the resulting solid was washed with the corresponding alcohol. All experiments were carried out at room temperature 24 °C ± 1 °C. The solids were kept dry and isolated from humidity at all times. X-ray diffraction data were obtained within 30 min after sampling. Tests were made to ensure that the samples had not changed with time before analysis.

X-ray diffraction data were obtained using a Bruker D8 Advance diffractometer with a scan range from 5 to 75° 2θ and a step size of 0.018° 2θ. The $K_{\alpha 2}/K_{\alpha 1}$ ratio was 0.5. The relative percentages of the polymorphs were derived by Rietveld refinement using TOPAS software version 4.2 (copyright 1999−2009 Bruker AXS). The goodness of fit average obtained was 1.8, and the calculated standard deviation for each polymorph in a mixture was <0.25%. Scanning electron microscopy (SEM) images were obtained on a Quanta 200F with a field emission gun (FEG). Samples were coated with 2−3 nm of Au or Pt/Pd and imaged at a working distance of 3−4 mm at 2 to 3 keV.

RESULTS AND DISCUSSION

Polymorph Discrimination As a Function of Type and Concentration of Alcohol. In all experiments, immediately after mixing the starting solutions, a white precipitate formed. On the basis of the lack of Bragg peaks in the X-ray diffraction (XRD) patterns, this precipitate was identified as amorphous calcium carbonate (ACC).[4] After 1 h of reaction, and regardless of physical and chemical conditions, all ACC transformed into one or more of the $CaCO_3$ polymorphs (calcite, vaterite, aragonite). The relative proportions of the phases, determined by refinement of the XRD data for all experiments, is shown in the ternary diagram (Figure 1). Polymorph proportion as a function of time is listed in Table 1, and the detailed, time-resolved XRD patterns for typical experiments are presented in Figures S1−S3 in the Supporting Information.

10% Alcohol, Gentle Shaking (GS). In the GS experiments with 10% ethanol, calcite was the dominant and final precipitate. The proportions in the assemblage evolved from proportions of calcite > vaterite > aragonite at 1 h to 100% calcite within 1 week (Table 1). After 5 h of reaction, ∼5% and 13% aragonite and vaterite were found, while after 1 day, only 1% of the sample was aragonite; the rest had transformed to calcite. Vaterite was not observed in the XRD refinement of the 1 day samples because the XRD detection limit is 1−2%, but in some of the SEM images, a few vaterite aggregates were observed.

dx.doi.org/10.1021/cg2012342 | Cryst. Growth Des. 2012, 12, 842−853

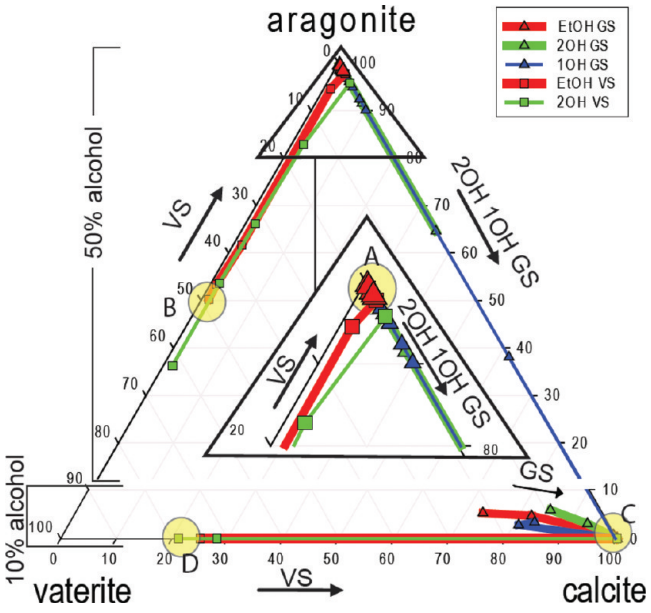

Figure 1. Phase diagram for calcite, aragonite, and vaterite, showing the relative percent of each polymorph derived from the Rietveld refinement of the XRD data. Each corner in the ternary diagram represents 100% of one of the three $CaCO_3$ polymorphs. The relative proportions of the polymorphs produced under each experimental regime (10% or 50% alcohol, GS (gentle shaking), or VS (vigorous shaking) and ethanol or 1-propanol (1OH) or 2-propanol (2OH)) are plotted as individual symbols. The symbols for each regime are joined by lines illustrating the polymorph evolution through the duration of the experiments (i.e., 1 h to 4 months). The yellow circles labeled A–D represent examples of points used for pinpointing experimental conditions that can be used to obtain specific desired polymorph ratios.

Polymorph evolution for this set of conditions (ethanol, GS) is illustrated in Figure 1 by the short red line close to the calcite corner, where the first point (triangle symbol at left end) represents the 1 h sample containing 21% vaterite, 5% aragonite, and 74% calcite. As the transformation progressed (i.e., 5 h, indicated by the second triangle on the red line), the proportion of calcite increased at the expense of vaterite, but a tiny portion of aragonite remained. In these GS experiments with 10% alcohol, the type of alcohol (ethanol, 1-propanol, or 2-propanol) did not have much of an influence on the polymorph distribution or pathway. This is demonstrated in Figure 1, where the red, blue, and green lines with triangle symbols close to the calcite corner can be compared. In all three alcohol systems, vaterite and aragonite formed initially, but transformed to calcite within a day. In terms of vaterite stabilization effect, ethanol was slightly more effective than 1-propanol and 2-propanol (Table 1, Figure 1).

50% Alcohol, Gentle Shaking (GS). In contrast, in the GS experiments with 50% ethanol, aragonite dominated over the full experimental range at more than 98% (Table 1). Vaterite was completely absent, and only small proportions (<2%) of calcite were observed. Hence the samples from these experiments plot in the aragonite corner on the calcite–aragonite line (red triangles, inset in Figure 1).

In the experiments with 50% alcohol, there was a clear difference in polymorph distribution between the three simple alcohols. Aragonite was most stable (i.e., present for the longest period of time) in the ethanol experiments and less so in the 1-propanol experiments. In the 1 h samples for all alcohols,

Table 1. Time Dependent Relative Proportions of the Polymorphs: C, Calcite; A, Aragonite; V, Vaterite Derived from Rietveld Refinement[a]

		10%			50%		
		C	A	V	C	A	V
GSH							
EtOH	1 h	74	5	21	2	98	
EtOH	5 h	82	5	13	1	99	
EtOH	1 d	99	1			100	
EtOH	1 w	100			1	99	
EtOH	1 m	100			1	99	
EtOH	4 m	100			2	98	
2OH	1 h	85	6	9	2	98	
2OH	5 h	93	3	4	8	92	
2OH	1 d	100				100	
2OH	1 w	100				100	
2OH	1 m	100			4	96	
2OH	4 m	100			35	65	
1OH	1 h	84	3	13	5	95	
1OH	5 h	81	3	16	3	97	
1OH	1 d	100			8	92	
1OH	1 w	100			10	90	
1OH	1 m	100			62	38	
1OH	4 m	100			100		
VSH							
EtOH	1 h	25		75	1	50	48
EtOH	5 h	25		75	1	53	46
EtOH	1 d	100			2	62	37
EtOH	1 w	100			1	95	4
EtOH	1 m	100			2	98	
EtOH	3 m	100				100	
2OH	1 h	21		79	2	36	62
2OH	5 h	28		72	2	54	45
2OH	1 d	100			2	66	32
2OH	1 w	100			2	83	15
2OH	1 m	100			4	96	
2OH	3 m	100			4	96	

[a]EtOH, 1OH, and 2OH correspond to ethanol, 1-propanol, and 2-propanol.

more than 95% of the precipitate was aragonite and vaterite was always absent. However, after 1 month of reaction, the relative polymorph percentages differed significantly: in the experiments with 1-propanol, aragonite had started to transform to calcite and only 38% aragonite remained. In contrast, more than 95% of the precipitate in the ethanol and 2-propanol experiments was still aragonite. After 4 months, the initial aragonite in the 2-propanol experiments had begun to transform to calcite, but the product was still dominated by 65% aragonite (green triangles in Figure 1). The 1-propanol samples after 4 months only contained calcite (blue triangles), while in the samples from the ethanol experiments aragonite remained the only phase, and thus plots (as red triangles) in the aragonite apex in Figure 1.

Vigorous Shaking, 10 and 50% Ethanol and 2-Propanol (VS). The experiments performed at vigorous shaking speeds (VS) produced a significant change in polymorph ratio compared with the experiments at gentle shaking speed (GS). In the 1 h samples with 10% ethanol, the vaterite proportion had increased from 21% and to 75% by increasing the shaking speed from 80 to 140 rpm. All 10% experimental regimes followed a classic vaterite to calcite

dx.doi.org/10.1021/cg2012342 | Cryst. Growth Des. 2012, 12, 842–853

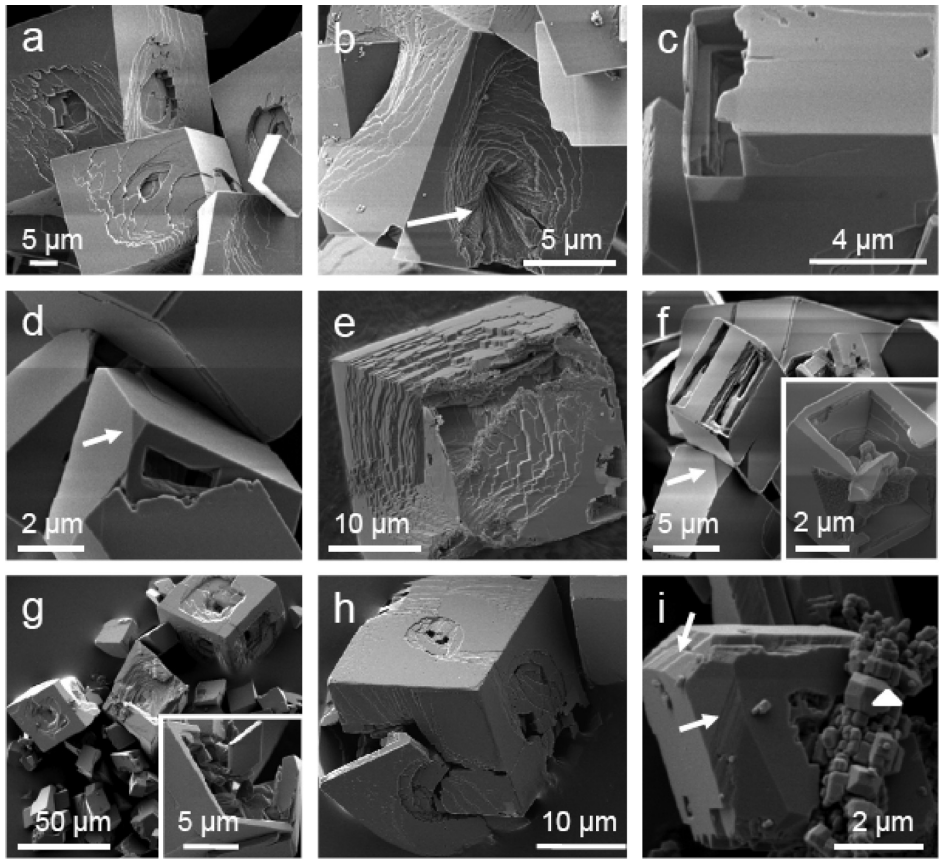

Figure 2. Morphology for calcite crystals precipitated in the GS experiments with 10% (a–h) and 50% (i) alcohol. (a) 1 h, hopper crystals and perfect rhombs; (b) 5 h, imprints of dissolved aragonite (arrow); (c) 1 day, cavities in the calcite crystal were found throughout the sampling interval, also seen in (d, e, f, g, and h); (d) 1 week, illustrates corner faces and cavities in rhombs; (e, f) 1 month; (e) calcite with a high step density and a corner cavity. The high step density is probably the remnant after vaterite or aragonite that was attached, and that served as a source for the growing calcite crystal; (f) rhombs with corner faces (arrow) and cavities; the inset shows a hollow crystal; (g, h) 4 months; calcite morphology still resembles that found in the 1 week samples; (i) in the VS experiments, the calcite in the 1 h to 1 week samples look like imperfect rhombs or hopper crystals as in (a). However, all the calcite observed in the 3 month samples had developed faces on crystal edges (arrows).

transformation profile where the vaterite had transformed to calcite within a day[4] (Table 1). In solutions of 50% ethanol or 2-propanol, the main reaction products were vaterite and aragonite with minor calcite (<4%). It is noteworthy that, and in contrast with the GS experiments, vaterite formed and was present for as long as a week when samples were vigorously shaken, in the presence of 50% alcohol. Compared with the phase proportions from the 10% alcohol GS data, which plotted close to the calcite corner in Figure 1, vaterite and calcite are produced in the 10% VS experiments, so they plot most of the way along the vaterite–calcite axis (red and green squares). Finally, in the presence of 50% alcohol, the phase fractions from the VS experiments plot on the vaterite–aragonite axis (red and green squares) compared with data from the GS experiments, that plot on the calcite–-aragonite axis (Figure 1).

The results clearly demonstrate that the type and proportion of alcohol, as well as the shaking speed, affect vaterite formation and stability. In the 10% GS experiments, most of the vaterite transformed to calcite within 1 day, but in the 50% VS experiments, some vaterite was still observed a week later, indicating a strong stabilization of this phase by the high alcohol percentage (Table 1 and Figure 1). In the 50% ethanol and 2-propanol experiments, vaterite transformed to aragonite after 1 month (Table 1), and this transformation pathway is illustrated on the vaterite–aragonite axis of Figure 1.

Alcohol Induced Morphology Control. The basic morphology for each of the polymorphs obtained in the three different alcohol systems, regardless of shaking regime, was roughly equivalent, and hence only images from the ethanol system are presented in Figures 2–4. The polymorphs that precipitated in our experiments are not markedly different from what is reported in other studies of $CaCO_3$ precipitation with and without alcohols or other additives (discussed in detail below), but they illustrate that even 10% alcohol has a marked influence on morphology compared with an alcohol free system.

Calcite. SEM images from the GS experiments with 10% alcohol show idiomorphic calcite rhombohedra and crystals with hollow sides (Figure 2a,g). Dimensions along the long axis range from 5 to 30 μm. Dickinson and McGrath[15] reported similar morphologies and described the crystals with hollow sides as shallow (Figure 2a) and deep (Figure 2g) pitted hopper crystals. Some of the calcite crystals are intimately connected with vaterite or aragonite (Figures 3b and 4a–c). In the 5 h samples, casts of dissolved aragonite can be seen (Figure 2b, arrow) and the calcite crystal, where the aragonite was attached, has a high step edge density (e.g., Figure 4c). In the 1 day samples, some of the calcite crystals have cavities (Figure 2c), and a variety of such cavities were found at several sampling intervals (Figure 2d–h). After 1 day, some of the

dx.doi.org/10.1021/cg2012342 | *Cryst. Growth Des.* 2012, 12, 842–853

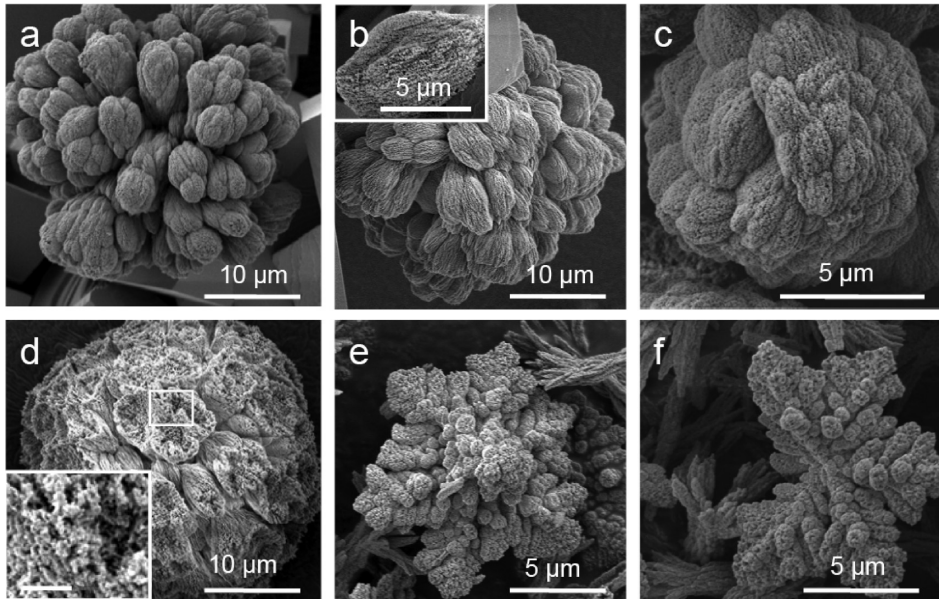

Figure 3. Morphology for vaterite obtained from experiments with 10 and 50% alcohol. With 10% alcohol, the morphologies are independent of shaking speed (a–d): (a, b) cauliflower and layer cake (inset in b) crystals form in the GS regime after 1 h. Calcite crystals are often attached to the vaterite clusters, as seen in a and b; (c) VS regime after 1 h showing more porous vaterite cauliflower structures; (d) during the vaterite to calcite transformation, the cauliflower spheres become corroded (the scale bar in inset is 1 μm); (e, f) dendritic vaterite precipitated in the VS experiments with 50% alcohol and sampled after 5 h; aragonite needles are present in both images.

calcite crystals developed faceted corner faces (Figure 2d, arrow); such faces were observed throughout the sampling period (Figure 2f, arrow).

Unfortunately, the extent of the corner faces is negligible relative to the dominating[31] faces, so their proportion is too low to be recognized in the XRD profile refinement. We interpret this face to be {11.20}. It is interesting that de Leeuw and Parker[32] determined from atomistic simulations that this face has the highest hydration energy among all of common faces of calcite. We presume that the same is valid for the adsorption of ethanol onto this face, leading to its enhanced stabilization. In the VS experiments with 10% alcohol, only a few hollow crystals were observed and there were no hopper crystals. In the VS experiments with 50% 2-propanol and ethanol, a few calcite crystals were identified in the SEM images in samples collected after 3 months (Figure 2i). The calcite shows facets on the rhombohedral edges that were not observed in the 10% experiments.

Vaterite. In the experiments with 10% alcohol, regardless of shaking speed, vaterite was mainly present as cauliflower-shaped spherical aggregates, but layer cake stacks in ellipsoidal clusters were also observed (Figure 3a–d). The cauliflower aggregates ranged in diameter from ~10 to 40 μm and often consisted of groups of pellets, which were globular clumps of irregular stacks of plates with thickness ranging from 1 to 5 μm. The pellets radiate from the center of the spherical aggregates and widen away from the center. The spherical aggregates have two voids located perpendicular to the radiation plane of the plates. The transformation from vaterite to calcite, documented by the XRD results (Table 1), was confirmed by the SEM images (Figure 3d), where the vaterite stacks have been extensively corroded, a process that was especially apparent in the nanometer scale subunits that make up the stacks (Figure 3d inset).

In the 50% alcohol, VS experiments, the morphology of vaterite was dramatically modified. Spheres gave way to flatter, dendritic clusters with a snowflake shape, indicative of fast growth (Figure 3e,f).[33] The dendritic clusters were 5–15 cm in diameter, with crystallites in the sub-micrometer range.

Aragonite. The crystals formed in 10% ethanol in the GS regime clustered as bundles of branching needles that radiate out from the calcite crystals that they are associated with (Figure 4a,b). The needles are composed of individual small segments that are on the order of 10–200 nm long. At these conditions, after 5 h of reaction, the dissolution of the aragonite bundles was pronounced, and the remaining segments had become less defined (Figure 4c), which paralleled transformation to calcite (Table 1).

The crystals composing the aragonite needles in the experiments with 50% alcohol (Figure 4d–i) were well-defined and after a week, some segments had grown at the expense of others by Ostwald ripening. This process continued throughout the experiment, producing inhomogeneous sizes for the segments of the individual needles (Figure 4g–i). Figure 2i shows aragonite crystals closely associated with calcite crystals after three months in VS experiments with 50% ethanol. The individual segments in the aragonite needles vary significantly in size, and the larger crystals developed {021} faces (Figure 2i triangle). The close association with calcite and the rhombohedral crystal form indicates that aragonite transformed to calcite. As for all other polymorphs, the shaking speed had little or no influence on aragonite morphology. The only effect of shaking speed on aragonite morphology was a thickening of the bundles.

Pathway for Synthesizing $CaCO_3$ with a Specific Polymorph, Ratio or Morphology. A simplified overview of the temporal evolution of the polymorph morphologies produced in solutions containing ethanol at 10% and 50% is presented in Scheme 1. By combining the information in Figure 1 and Scheme 1, morphology was integrated into the framework of experimental variables. This way, the optimal experimental parameters for synthesizing a product with a

dx.doi.org/10.1021/cg2012342 | Cryst. Growth Des. 2012, 12, 842–853

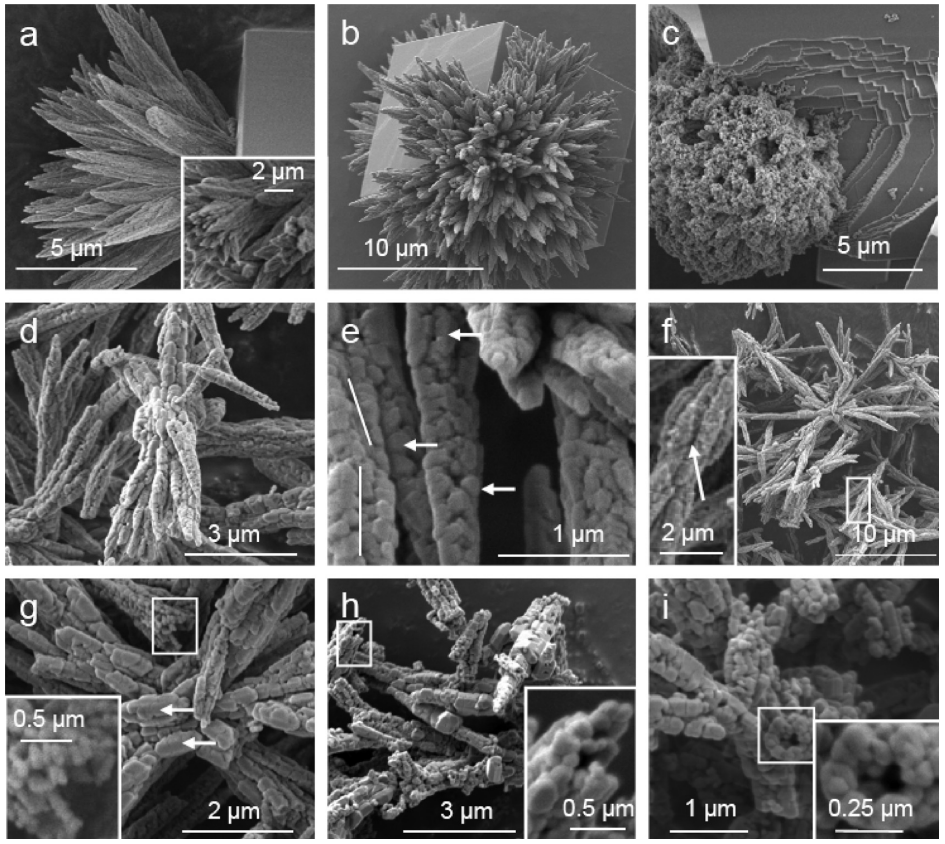

Figure 4. SEM images of aragonite precipitated in the experiments with 10% (a–c) and 50% (d–i) alcohol. (a, b) Aragonite associated with calcite sampled after 1 h, with the aragonite branching irregularly; (c) dissolution of the aragonite is ongoing in the 5 h samples; (d) in the 1 h samples with 50% alcohol, the aragonite needles branch and form bundles (sheaves); (e) most individual segments (arrows) are separated by horizontal and subvertical winding seams (lines) and striations or grooves perpendicular to the needle length. (f) Aragonite sheaves after 5 h, some consisting of protruding ribs and grooves parallel to the needle axis (inset, arrow); (g) after 1 day, some of the individual segments have grown larger (arrows). Broken needles reveal a central cavity (inset); (h, i) after 4 months, Ostwald ripening has caused some segments to grow larger at the expense of others and some of the seams that had separated the earlier crystals had disappeared or had been hidden by overgrowth. Central cavities and a pseudohexagonal symmetry can be recognized (insets).

Scheme 1. Simplified Morphological Evolution with Time for the Various Experimental Regimes for Ethanol Solutions[a]

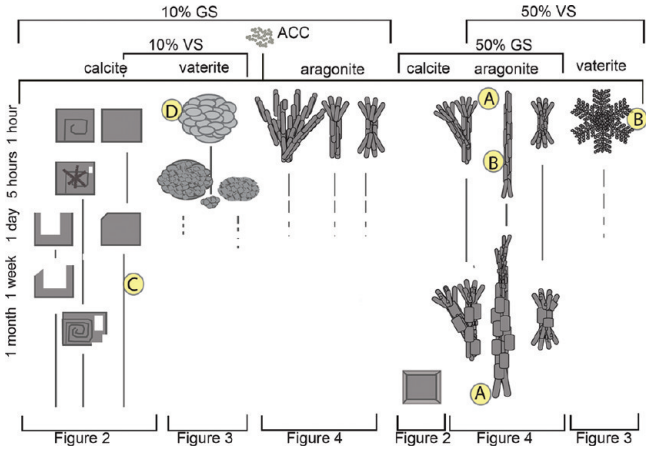

[a]The roughly 2% calcite in the 50% GS experiments has been assumed to be irrelevant. The letters in shaded circles refer to examples of constrained experimental condition that could be used for synthesizing specific polymorph ratios. These are equivalent to the same points illustrated in Figure 1. The crystal sketches are not to scale.

particular polymorph ratio or morphology could be derived (Table 1, Scheme 1). For example, our results suggest that we could expect nearly 100% aragonite from experiments with 50% ethanol and gentle shaking from samples reacted for 1 h to 4 months (Table 1 and Figure 1 point marked with A) showing that the product was not sensitive to time in solution. If the aim was to produce a 50:50 aragonite/vaterite mix, the best strategy would also be 50% ethanol, but with vigorous shaking and a reaction time of only 1 h (point B in Figure 1 and Scheme 1). The vaterite formed would be expected to be in dendritic clusters (Scheme 1B), while the aragonite would be long, composite aggregates. For pure calcite, one would sample after one week from solutions with 10% alcohol (Figure 1 and Scheme 1 point C), while for a high amount of cauliflower vaterite, one should stop the reaction after 1 h in solutions with 10% 2-propanol and vigorous shaking (Figure 1 and Scheme 1 point D).

It is well-known that vaterite and calcite mixtures can be produced in a pure system, that is, without alcohol. Hence, for industrial purposes, we anticipate that the most interesting mixtures precipitated in our studies would be aragonite and dendritic vaterite. We propose an equation for estimating the time needed for obtaining specific aragonite–calcite or aragonite–vaterite mixtures. The equation (eq 1) has been

dx.doi.org/10.1021/cg2012342 | Cryst. Growth Des. 2012, 12, 842–853

derived from the results of our experiments in the 50% 1-propanol with GSH and 50% ethanol with VSH only, and we acknowledge that this equation is made from a limited data set. The full data sets and fit parameters are presented in Supporting Information. The equation reveals that for sampling time, x in hours (1 month = 672 h) can be calculated via

$$x = \frac{127.37 - v}{0.1579} \ln\left[\frac{0.0207(y - 100)}{r - 4.2345}\right] \quad (1)$$

where v denotes the shaking speed (revolutions per minute, RPM), r is the alcohol/water mole ratio and y represents the % aragonite in the product.

The equation is based on the constraints provided in Table 2. That is, the proportion of aragonite, y, that can be predicted

Table 2. Constraints for the Range and Use of eq 1

constraints	50% 1-propanol	50% ethanol
range (% aragonite)	40–95	50–100
polymorphs	aragonite–calcite	aragonite–vaterite
RPM (revolutions per minute) (v)	80	140
alcohol/water ratio (r)	4.1	3.2

with this equation ranges from 40 to 95% for the aragonite–calcite mixture and 50–100% for aragonite–vaterite mixtures. A corresponding equation for the production of optimal calcite/vaterite mixtures in the presence of alcohols was not derived because it is equivalent to that in the pure system.[4]

Growth Mechanism. *Calcite.* In aqueous systems, hopper crystals of calcite form at intermediate to high saturation index SI,[34,35] and as SI decreases, the cavities fill as the crystals grow by screw dislocation, smoothing the faces. This process is well-known and explains most of the crystal form evolutions observed here. However, the voids in the calcite crystals and the extra face are not observed in the pure system (Figure 2b,d,f) and are interpreted to be a consequence of the presence of alcohols.

In Figure 2b (arrow), the large crater is a clear remnant mold of previous aragonite and the hollow calcite crystals (Figure 2c–h) only appear from experiments where polycrystalline aragonite was originally present. Hence, we interpret that the observed cavities are remnants of dissolved aragonite where the calcite has crystallized on the initially rough aragonite surface. Our SEM images show that aragonite and vaterite are intimately associated with calcite (Figures 3b and 4a–c). If calcite overgrows aragonite clusters using Ca and CO_3 from the dissolving aragonite, material is preferably deposited on the outside. When dissolution of the aragonite was complete, insufficient material was available close by for filling the central cavity. Most of the ions from the surrounding solution would attach at the external corners of the crystal and be unable to reach the internal cavities, so the hollow crystal faces would persist. Imprints of original vaterite in growing calcite are known from pure system studies and are a consequence of the surface driven dissolution of vaterite from which calcite grows.[4] In the pure system, such imprints heal within hours whereas in the alcohol inhibited experiments, imprints and cavities were observed throughout the entire sampling period.

Aragonite and Vaterite. In this study, the crystal forms observed for both aragonite and vaterite are similar to those reported from a variety of other experiments with and without additives. For aragonite, Zhou et al.[36] reported "mesoscale hierarchical rods of aragonite" formed in an additive free system and the authors called them "mesocrystals". Some of the rods were bent and some had interior cavities and multi or Y branched structures. Zhou and colleagues argued that the porous structure and slight misorientation were evidence for oriented attachment where separate, individual nanoparticles spontaneously aligned themselves. In a system containing pyrrolidone, Shi et al.[37] reported formation of "rosette superstructures" that they interpreted to have developed from small, needle-like particles that evolved into shuttles, rods, and finally sheaf or dumbbell shapes through parallel aggregation.

The aragonite needles that formed in our experiments generally have a pseudohexagonal morphology (Figure 4e arrow, g–i inset), where each needle is composed of small segments separated by well expressed, perpendicular grooves. In the majority of cases, each face of the needles has irregular, subvertical winding seams along its central line (i.e., Figure 4e, line) that mark the contacts of the segments. The sequence of such contacts, for differently sized individual segments along the length of the needle, produces the winding seam. The domains are individualized to a different degree, from semicontinuous ribs, forming edges of the needle (i.e., Figure 4f, arrow) to sequences of blocky segments of somewhat different sizes (i.e., Figure 4e,g, arrows). The ribs convert into sequences of coarser, well faceted segments with time, a process we consider to be the result of crystal growth and thickening of individual domains in the process of Ostwald ripening. Broken needles reveal a central void and confirm that each edge of the pseudohexagonal needle represents an individual crystal (Figure 4i, inset). Comparison of the crystal form observed in the SEM images with large natural aragonite crystals[38] leads to the conclusion that the vast majority of the needles are composite aragonite twins, where each needle face corresponds to {110} faces, from two distinct, adjacent twin individuals (Figure 5a).

Aragonite has an orthorhombic crystal structure, where the calcium layers and CO_3 layers are parallel to (001) in a pseudohexagonal arrangement.[39] Aragonite habitually forms pseudohexagonal cyclic twins, with three (I, II, and III) orientations of component individuals produced by twinning on the {110} symmetry planes (Figure 5a). The a axis of each individual emerges through the edge of the needle, perpendicular to the needle axis. The geometry of the pseudohexagonal prisms of aragonite develops from the first contact twin of two individuals, obtained by reflection on (110), with the a axes meeting at an angle of 116.18° instead of the ideal hexagonal value of 120° (Figure 5b). The next twin individual attaches itself in the same manner to the first or to the second crystal (Figure 5d). Overgrowing to the opposite side, these three orientations produce together the interpenetration twin in which each regularly twinned pair produces an angle of 63.82° between a twin individual and an overgrowth portion of another individual (Figure 5b). We have made these calculations using the new aragonite lattice data of ICSD 52152; it would be complicated to derive this data from the crystals produced in our experiments, because the very small size and intergrowth makes it difficult to measure the angles with precision.

One case where individual I is twinned with individual II, and then II is twinned to III is illustrated in Figure 5e. Black individual I twins to bright gray individual II, which twins with dark gray individual III. Because the twinning angle between the black and bright gray units is 116.18°, the angle between a

dx.doi.org/10.1021/cg2012342 | Cryst. Growth Des. 2012, 12, 842–853

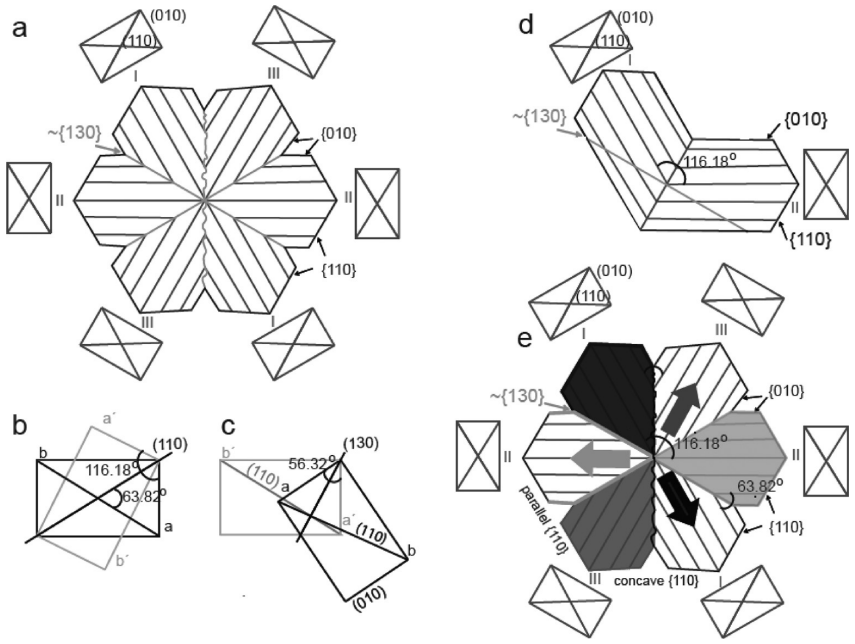

Figure 5. Aragonite twinning model. (a) Aragonite twinning viewed along (001), modified from Bragg.[39] The rectangles represent unit cell orientations; (b) twinning on the (110) twin plane represented by unit cells of aragonite; (c) twinning along the nontwin plane (130); (d) twinning of crystal I to II along (110); (e) twinning of crystal I (black) to II (light gray) and II to III (dark gray) and the subsequent overgrowth of the material (arrows) producing an intergrowth twin.

bright gray individual and the overgrown portion of I is 63.82°. This is similar for the twinning of bright gray to dark gray. This systematic, however, leaves only 52.36° between the individuals not related by twinning (i.e., black and dark gray individuals). The contacts at 63.82° produce pairs of exactly parallel {110} faces, but the forced contact of individuals not related by twinning results in two concave faces on the opposite sides of the twin (Figure 5e).

Contacts of adjacent individuals in the interpenetration twin appear to be the {130} planes (Figure 5a,e). However, the {130} plane is not a twinning plane in the aragonite structure, so it would produce unfavorable O−O distances for such an operation. Calculations show that the *a* axes of two crystals twinned on {130} would produce an angle of 56.32° (Figure 5c) instead of the observed 63.82°. The {130} planes in the interpenetration twin diverge by 7.5°, illustrating that the contact plane is not a plane with simple Miller indices.

A primary cyclic twin with a geometry based on {110} twinning and a hollow center which prevents formation of the penetration cannot exist because of the inevitability of the ~{130} contacts in it. Without the interpenetration scheme that follows from the {110} twinning, the orientation of component individuals collapses. Contact on exact {130} planes would result in a sidewise open tube with a gap of 18°. Thus, we suggest that the twin aggregates of aragonite started as short prismatic interpenetration twins with a pseudohexagonal outline and the central cavity results from solutions starved of their Ca^{2+} and CO_3^{2-} because they had been deposited on the outer, fast growing surface of the tube. Occasional inner contacts in the tube interior would have helped to maintain the orientation of component individuals.

Although rapid crystallization has favored needle growth, the individualization of needle edges into sequences of stubby domains by frequent occurrence of (001) and, perhaps, (111) faces could be connected either with the occurrence of stacking faults in the aragonite structure or with blocking of (001) faces by absorbed molecules. These explanations, and the explanation of primary interpenetration prisms described above, can be compared with the morphology of the aragonite material synthesized by Krauss et al.[40] through electrochemical deposition in the presence of Mg^{2+} and by Liu et al.,[41] who crystallized aragonite from stirred solutions at pH 8 in the presence of Ca- and Mg-dodecyl sulfate at 60 °C. They also obtained stubby pseudohexagonal prisms with prominent (001) faces, with traces of multiple twinning and with steps on vertical faces similar to our case. The prismatic habit with (001) pinacoids corresponds to the morphology of aragonite that grows in fine sediments.

For vaterite, the cauliflower morphology observed in this study parallels descriptions in the literature in both the pure and the alcohol containing systems. For example, Zhou et al.[42] precipitated vaterite with a wide range of morphologies, including cauliflower spheres, by varying pH, Ca/CO_3 ratios and temperature, without using alcohol. Furthermore, Manoli and Dalas[16] reported the development of two different types of cauliflower spheres by varying the type of alcohol (ethanol, isopropanol, and diethylene glycol), and Zhang et al.[24] reported that cauliflower vaterite formed in the presence of ethanol but accompanied by aragonite. They concluded that by varying the Ca/CO_3 ratio, they could define the relative proportions of aragonite and vaterite. Andreassen[27] reported cauliflower vaterite in experiments with no alcohol, but carried out at a higher temperature (50 °C) where the resulting vaterite formed wider pellets on the cauliflower aggregates. Simpler vaterite cauliflowers with thin and unbranched pellets were grown on vaterite seed by Beck and Andreassen[28] while Zhang et al.[43] used solutions containing *p*-aminobenzene sulfonic acid anhydrous and L-lysine complexes.

The cauliflower morphology is typical for vaterite, but there are several hypotheses for the mechanisms responsible for its formation. Many of them favor nanoaggregation. Zhang et al.[43]

dx.doi.org/10.1021/cg2012342 | *Cryst. Growth Des.* 2012, 12, 842−853

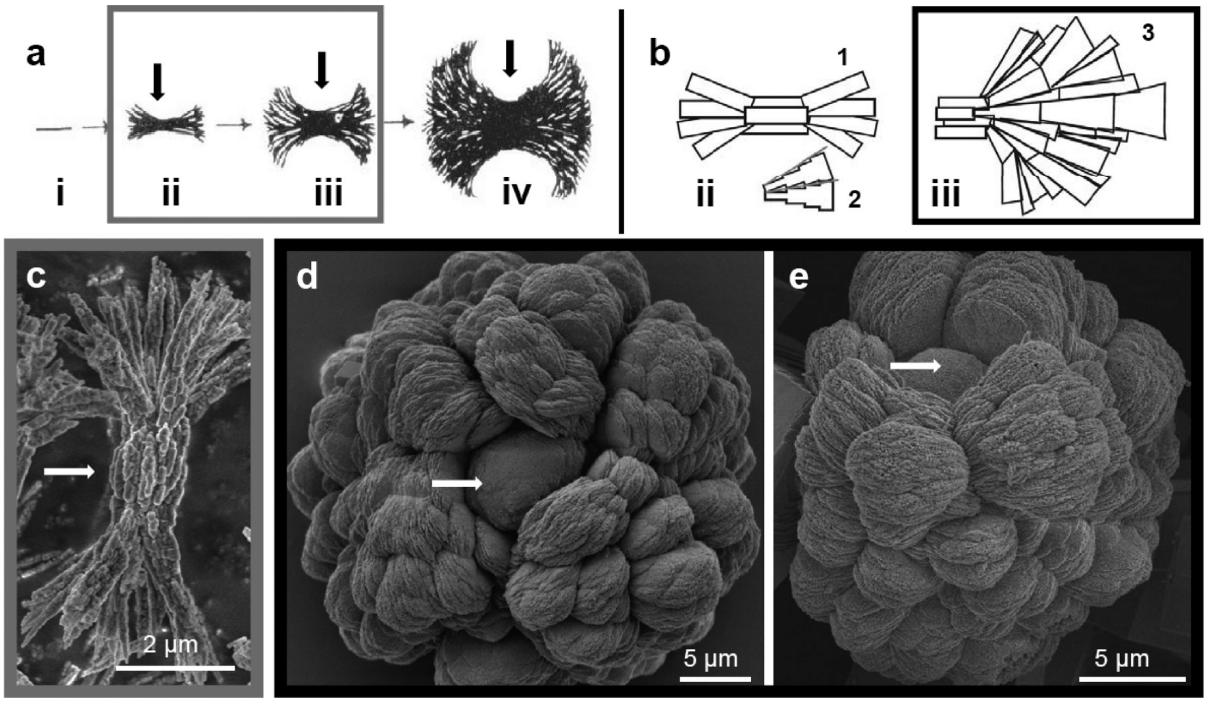

Figure 6. (a) Category 2 spherulitic growth models modified from Granasy et al.;[45] (b) schematic models of spherulitic growth of vaterite, (1) illustrative model of spherulitic growth of platelets, (2) more realistic morphology of the individual asymmetric platelets, (3) our favored model of spherulitic growth of vaterite (only half spherulite is shown) where the asymmetric platelets create new growth sites and develop the divergence of platelets along the a direction; (c–e) morphology of (c) aragonite sheaves and (d, e) the cauliflower-shaped spherical aggregates of vaterite. Development of aragonite corresponds to stages (a) i–iii, that of vaterite, stage (b) iii. Arrows indicate "eyes".

speculated that surfactants, adsorbed on clusters of several ACC grains, could orient them to trigger formation of several forms of vaterite. Chen et al.[8] proposed that layer cake vaterite crystals form as precipitates on CO_2 bubbles and then these aggregate and recrystallize. Gehrke et al.[44] precipitated vaterite in the presence of ammonia. The morphology was simpler, thin, unbranched pellets, similar to that reported by Zhang et al.[43] and Andreassen,[27] so they argued for a three-dimensional oriented attachment of individual vaterite nanoparticles. However, Andreassen[27] concludes that it would take orders of magnitude higher supersaturation to obtain the particle numbers required for such an aggregation of nanoparticles. Andreassen[27] and Beck and Andreassen[28] argue that vaterite is the result of spherulitic growth and hence spheres originate from one single crystallization event, not the consequence of nanoparticle aggregation.

Spherulitic Growth. Models for spherulitic growth have been described by Granasy et al.,[45] who used phase field modeling to propose two main types: Category 1 spherulites, originating at a single point nucleation site, where the crystallites have arms that grow radially, branching irregularly to fill all of the space available and Category 2 spherulites, that initially grow as parallel fibers, leading to formation of new crystallites at the growth front (Figure 6a). Branching leads to a crystal sheaf that increasingly splays out and eventually develops two eyes, which are void regions on each side of the primary nucleation zone. Ultimately, this type of spherulite settles into spherical shape with remnant eye structures in its core region (arrows in Figure 6a). Traditionally, spherulitic growth is associated with viscous solutions, but Granasy et al.[45] described a mechanism of noncrystallographic branching that takes place in low viscosity systems. In that case, fibrils form at a fixed supersaturation and secondary fibrils nucleate at a growth front to form crystal sheaves. The diverging ends of these sheaves subsequently fan out with time and can form a roughly spherical particle (Figure 6a).

In our understanding of the formation of spherulites, the newly created nuclei on, or attached to, the growing surface are subjected to a Darwinian selection concerning their orientation, or misorientation, with respect to the growing aggregate. All nuclei that are not aligned with the fastest growing direction of the expanding surface are eliminated and growth results in essentially parallel needles or plates. At the edges of the growth front, however, misoriented nuclei can grow, and their growth is enhanced because the free perimeter of the growing aggregate faces a continuous supply of material from the solution. This process can produce increased branching of crystals with either needle or platelet morphology and can lead to formation of sheaves and dumbbells, such as those shown in Figure 6.

The aragonite aggregates and the cauliflower vaterite spheres produced in our experiments parallel the morphologies for category 2 spherulites described by Granasy et al.[45] (Figure 6a). Figure 6a shows the development of spherulitic growth of acicular crystals as described by Granasy et al.,[45] and applies directly to the aragonite needles. The vaterite that consists of platy, rather than acicular building blocks has a similar development of the spherulitic growth as aragonite, with platelets rather than fibers diverging, and is sketched in Figure 6b. In addition, the SEM images indicate that the vaterite platelets get thicker outward, toward the solution because of the supply of building ions (Figure 6b2) rather than the simple model of constant platelet thickness shown in Figure 6b1. We propose that this asymmetry of the platelets influences the attachment mode of new platelets (Figure 6biii for a half spherulite) and enhances the statistical divergence of the

dx.doi.org/10.1021/cg2012342 | *Cryst. Growth Des.* 2012, 12, 842–853

platelets. For both the aragonite and the vaterite models, divergence of needles or platelets is possible toward the empty side of the growth front but not to the side that is occupied by other growing needles or platelets. As a consequence, the *c* directions of aragonite needles diverge, whereas their *a* directions converge into the "eye" (black arrows in Figure 6a). For vaterite the *a* directions diverge and the *c* directions converge into the "eye". Figure 6c−e shows the aggregates of vaterite and aragonite obtained in our experiments. The morphology of vaterite matches the stage (b) iii and that of aragonite matches stages (a) i−iii in the top of the figure. Both aragonite and vaterite have developed "eyes" over the nucleus region (arrows in Figure 6c−e).

Classical or Nonclassical Growth. Precipitation through homogeneous nucleation, as in our experiments, influences the saturation index (SI) during reaction. At the point when two solutions mix, SI is high, and as precipitation proceeds, SI decreases, with an accompanying change in crystal form. For example, refs 33−35 at high SI, the driving force of crystallization is high and we expect to see spherulitic and dendritic growth and formation of hopper crystals.[33] As the SI drops, crystal faces grow from screw dislocations and fronts advance, filling the hopper crystal cavities and generating flat faces.[46] These processes describe the evolution of crystal formation following classical growth theory, and this fits the sequence of morphologies observed in this study. In samples from the 1 h experiments, where the polymorphs are formed in the high SI regime, we observe calcite hopper crystals and vaterite and aragonite spherulites. As SI decreases, vaterite transforms to calcite, and dissolution−precipitation proceeds to fill and extend the crystal faces.

An important result of our studies is that the crystal forms observed do not give any evidence to support the hypothesis of nanoparticle self-assembly. Aragonite needles and vaterite spherical aggregates have been produced in many other studies using various additives and experimental regimes. Thus these morphologies are not unique to a specific additive or set of conditions, and this implies that a common growth mechanism must exist. The spherulitic growth mechanism provides the simplest and most logical explanation for aragonite sheaf and vaterite cauliflower crystal forms that we observed and that Granasy et al.[45] have described. It is reasonable to assume that the width and thickness deviations of the single pellets of vaterite described in the literature are a consequence of the growth regime in the individual studies, that is, fast or slow growth (low or high SI). Finally, perhaps the most compelling evidence is that the formation of cyclic twins, of the type described here for aragonite, cannot be explained by oriented, or nonoriented, assembly of nanocrystals. If nanocrystals were attaching themselves, they would be expected to attach by twinning on, and adhesion to, the {110} face, and they would use any of the four twin orientations offered by twinning on a single initial crystallite, entirely at random, forming a rather chaotic, fine grained aggregate. They would not attach themselves on ∼{130} faces, as observed for the overwhelming majority of aggregates, because this is not a favored crystal plane for aragonite.

The Effect of Alcohol. The slow filling of hopper crystal cavities and the persistence of calcite crystals with cavities even after several months indicate that Ostwald ripening is slow in the solutions with 10% alcohol. An explanation can be drawn from some recent studies where calcite surfaces were examined in solutions containing ethanol and water. Cooke et al.[25] used molecular dynamics (MD) simulations and atomic force microscopy (AFM) and showed that ethanol adsorbs more strongly than water to the {10.4} calcite surface and that ethanol displaces adsorbed water. They also found that ethanol bonds to the calcite surface through the OH group oriented such that the CH_3 group points away from the surface creating a hydrophobic termination of the first adsorbed ethanol layer. These finding are supported by recent data from X-ray reflectivity.[47] In another study, calcite surfaces exposed to ethanol were examined using atomic force microscopy (AFM) and the results compared with molecular dynamics (MD) simulations.[48] The combined results revealed the molecular structure of the fluid−solid interface and that in 96% ethanol the structured layer stabilizes the terraces and forbids water aided ion transport except at steps and defect sites. It is therefore likely that ethanol also binds strongly enough to all $CaCO_3$ polymorphs, that even with water present, growth is inhibited on certain faces. At ethanol blocked surfaces, the transport of Ca^{2+} and CO_3^{2-} necessary for growth is hindered, slowing the rate of recrystallization.

Our data show that alcohol also has a clear influence on the polymorph distribution in the experiments. The surface energies of calcite and aragonite are similar, but Chen et al.[8] argued that they would not be equally affected by changed solvent composition because of the different atomic configuration that is exposed in the termination of the bulk structure in the two minerals. This could explain the prolonged aragonite stability in solutions at room temperature. The increased stability is likely to be caused by a stabilization of the surface rather than of the bulk. Chen et al.[8] proposed that adding alcohol to the solutions with Ca^{2+} and CO_3^{2-} ions would increase the SI of the solution. This is supported by our interpretation of the aragonite and vaterite morphology resulting from spherulitic growth. Whether the SI of the polymorphs in the solution is increased by increased activity of Ca^{2+} and CO_3^{2-} ions or by decreased solubility in the alcohol solution is not clear. The branching observed on the vaterite pellets in this study is not observed in the pure system, so the driving force of crystallization is enhanced by alcohol.

The difference in aragonite stabilization for the different simple alcohols observed in the 50% experiments could be a consequence of using volume percentages where we obtain a lower molar alcohol/water ratio with higher molar mass of the alcohol. The ratio of ethanol/water molecules in the 50% mixture is 1:3.2, whereas the propanol/water is 1:4.1 and the isopropanol/water is 1:4.2. That means that in ethanol solutions, there are proportionally more −OH groups from the alcohol compared with the propanol solutions. The differences in molar ratio are small however. The change could also be ascribed to the geometry of the molecule and the position of the OH group with respect to the hydrocarbon parts.

One of the major new results from this study is that shaking has a significant effect on the polymorph precipitated, but not on its stabilization with time (Table 1), which indicates that ethanol affects the physical parameters in the solution. Zhang et al.[24] investigated the alcoholization and hydration of Ca^{2+} and CO_3^{2-}, using molecular dynamics simulations. They reported that CO_3^{2-} ions in ethanol−water mixtures are mainly solvated by water and hardly dissolve in ethanol, whereas Ca^{2+} ions are solvated both by water and by ethanol. Their calculations also predicted that at high ethanol mole fraction (0.7), a two phase system exists. Guo et al.[23] used X-ray absorption and emission spectra of methanol, water, and mixtures of

dx.doi.org/10.1021/cg2012342 | *Cryst. Growth Des.* 2012, 12, 842−853

the two to investigate the influence of the intermolecular interaction on the local electronic structure. They reported incomplete mixing in water−alcohol systems and a strong component of hydrogen bonding. From the results of our experiments, we can speculate that in solutions shaken vigorously, solvent structuring is disrupted, leading to easier ion transport pathways and increased precipitation, thus changing the kinetics of vaterite-water interactions so calcite formation is inhibited. Dendrites, as we observed in the 50% VS experiments, usually occur in a regime with both high SI and high growth rate.[33] These results suggest that vigorous shaking hastened ion transport to the growing solid surface, causing dendritic growth.

CONCLUSIONS

The precipitatetd $CaCO_3$ polymorph, and its morphology, can be controlled by selecting specific formation conditions from an experimental matrix of simple alcohols, time, and shaking speed. Vaterite precipitation can be simply controlled with shaking speed. The dominance of aragonite or calcite can be adjusted with the amount of alcohol added and the time elapsed before sampling. At high shaking speeds, vaterite can form two distinct morphologies, polycrystalline cauliflower shaped spherical aggregates using 10% alcohol, or by adding 50% alcohol, dendritic flat aggregates. No difference in morphology could be demonstrated by the presence of simple alcohols. Hence the position of the −OH group on alcohol has no influence. The most important parameters were the amount of alcohol and the speed of shaking.

Investigations of morphology lead us to conclude that the polycrystalline aragonite needles and vaterite spherical aggregates were formed by spherulitic growth by classical, ion-by-ion attachment and not by self-assembly of nanocrystals. This interpretation is supported by the evolution of morphology with time for all of the polymorphs, which can be explained by classical growth theory. The pseudohexagonal aragonite needles are twin intergrowths, with twinning on the {110} plane and intergrowth contact on ∼{130} faces. The {130} face is not a twin plane and contacts such as these cannot be explained by the current theories of nanoparticle aggregation.

Although not a direct aim of this work, the results from experiments with alcohol emphasize that decreased water activity by addition of organic compounds provides a strong tool for organisms to use in controlling biomineral formation, where polymorph stabilization and engineered morphology are required.

ASSOCIATED CONTENT

Supporting Information

XRD patterns of the sampled $CaCO_3$ precipitates and the derivation of eq 1. This material is available free of charge via the Internet at http://pubs.acs.org.

AUTHOR INFORMATION

Corresponding Author

*Phone: +4535320219. Fax: +4535320322. E-mail: kks@nano.ku.dk.

ACKNOWLEDGMENTS

We sincerely thank Keld West, Joanna Nissenbaum, Klaus Bechgaard and the NanoGeoScience group from the University of Copenhagen (KU) for help and discussion; Caroline Hem (KU), Helene Almind (KU), and Pieter Boots (Universty of Leeds) for XRD analysis and TOPAS advice; Berit Wenzell and Zoltan Balogh from CEN, DTU for SEM training; and three very helpful anonymous reviewers. Funding was provided to KKS by the Nano-Chalk Venture, from the Danish National Advanced Technology Foundation (HTF), Maersk Oil and Gas A/S, and the UK EPSRC Framework Grant called MIB; funding for JDRB through a Marie Curie EU-FP6MINGRO Research and Training Network fellowships under Contract MRTNCT-2006-035488 is acknowledged.

REFERENCES

(1) Michel, F. M.; MacDonald, J.; Feng, J.; Phillips, B. L.; Ehm, L.; Tarabrella, C.; Parise, J. B.; Reeder, R. J. Structural characteristics of synthetic amorphous calcium carbonate. *Chem. Mater.* **2008**, *20*, 4720−4728.

(2) Ogino, T.; Suzuki, T.; Sawada, K. The formation and transformation mechanism of calcium-carbonate in water. *Geochim. Cosmochim. Acta* **1987**, *51*, 2757−2767.

(3) Bots, P.; Rodriguez-Blanco, J. D.; Shaw, S.; Benning, L. G. The effect of sulphate and magnesium on the formation and stability of vaterite. *Acta Mineral.-Petrogr.* **2010**, *6*, 825.

(4) Rodriguez-Blanco, J. D.; Shaw, S.; Benning, L. G. The kinetics and mechanisms of amorphous calcium carbonate (ACC) crystallization to calcite, via vaterite. *Nanoscale* **2011**, *3*, 265−271.

(5) Wray, J. L.; Daniels, F. Precipitation of calcite and aragonite. *J. Am. Chem. Soc.* **1957**, *79*, 2031−2034.

(6) Nassif, N.; Gehrke, N.; Pinna, N.; Shirshova, N.; Tauer, K.; Antonietti, M.; Colfen, H. Synthesis of stable aragonite superstructures by a biomimetic crystallization pathway. *Angew. Chem., Int. Ed.* **2005**, *44*, 6004−6009.

(7) Mann, S. *Biomineralization: Principles and Concepts in Bioinorganic Materials Chemistry*; Oxford University Press: New York, 2001.

(8) Chen, S. F.; Yu, S. H.; Jiang, J.; Li, F. Q.; Liu, Y. K. Polymorph discrimination of $CaCO_3$ mineral in an ethanol/water solution: Formation of complex vaterite superstructures and aragonite rods. *Chem. Mater.* **2006**, *18*, 115−122.

(9) Colfen, H. Precipitation of carbonates: recent progress in controlled production of complex shapes. *Curr. Opin. Colloid Interface Sci.* **2003**, *8*, 23−31.

(10) Han, Y. S.; Hadiko, G.; Fuji, M.; Takahashi, M. Crystallization and transformation of vaterite at controlled pH. *J. Cryst. Growth* **2006**, *289*, 269−274.

(11) Meldrum, F. C.; Colfen, H. Controlling mineral morphologies and structures in biological and synthetic systems. *Chem. Rev.* **2008**, *108*, 4332−4432.

(12) Sommerdijk, N. A. J. M.; de With, G. Biomimetic $CaCO_3$ mineralization using designer molecules and interfaces. *Chem. Rev.* **2008**, *108*, 4499−4550.

(13) Lowenstram, H. A.; Weiner, S. *On Biomineralization*; Oxford Press: New York, 1989.

(14) Mann, S.; Webb, J.; Williams, R. J. P. *Biomineralization: Chemical and Biochemical Perspectives*; VCH: New York, 1989.

(15) Dickinson, S. R.; McGrath, K. M. Switching between kinetic and thermodynamic control: calcium carbonate growth in the presence of a simple alcohol. *J. Mater. Chem.* **2003**, *13*, 928−933.

(16) Manoli, F.; Dalas, E. Spontaneous precipitation of calcium carbonate in the presence of ethanol, isopropanol and diethylene glycol. *J. Cryst. Growth* **2000**, *218*, 359−364.

(17) Seo, K.-S.; Han, C.; Wee, J.-H.; Park, J.-K.; Ahn, J.-W. Synthesis of calcium carbonate in a pure ethanol and aqueous ethanol solution as the solvent. *J. Cryst. Growth* **2005**, *276*, 680−687.

(18) Yan, G. W.; Wang, L.; Huang, J. H. The crystallization behavior of calcium carbonate in ethanol/water solution containing mixed nonionic/anionic surfactants. *Powder Technol.* **2009**, *192*, 58−64.

(19) Zhu, L. Y.; Zhao, Q. R.; Zheng, X. W.; Xie, Y. Formation of star-shaped calcite crystals with Mg^{2+} inorganic mineralizer without organic template. *J. Solid State Chem.* **2006**, *179*, 1247−1252.
(20) Dedonder-Lardeux, C.; Gregoire, G.; Jouvet, C.; Martrenchard, S.; Solgadi, D. Charge separation in molecular clusters: Dissolution of a salt in a salt-(solvent)(n) cluster. *Chem. Rev.* **2000**, *100*, 4023−4037.
(21) Dixit, S.; Crain, J.; Poon, W. C. K.; Finney, J. L.; Soper, A. K. Molecular segregation observed in a concentrated alcohol-water solution. *Nature* **2002**, *416*, 829−832.
(22) Dougan, L.; Bates, S. P.; Hargreaves, R.; Fox, J. P.; Crain, J.; Finney, J. L.; Reat, V.; Soper, A. K. Methanol-water solutions: A bi-percolating liquid mixture. *J. Chem. Phys.* **2004**, *121*, 6456−6462.
(23) Guo, J. H.; Luo, Y.; Augustsson, A.; Kashtanov, S.; Rubensson, J. E.; Shuh, D.; Zhuang, V.; Ross, P.; Ågren, H.; Nordgren, J. The molecular structure of alcohol-water mixtures determined by soft-X-ray absorption and emission spectroscopy. *J. Electron Spectrosc. Relat. Phenom.* **2004**, *137*−*140*, 425−428.
(24) Zhang, L.; Yue, L.-H.; Wang, F.; Wang, Q. Divisive effect of alcohol-water mixed solvents on growth morphology of calcium carbonate crystals. *J. Phys. Chem. B* **2008**, *112*, 10668−10674.
(25) Cooke, D. J.; Gray, R. J.; Sand, K. K.; Stipp, S. L. S.; Elliott, J. A. Interaction of ethanol and water with the $\{10\bar{1}4\}$ surface of calcite. *Langmuir* **2010**, *26*, 14520−14529.
(26) Colfen, H.; Mann, S. Higher-order organization by mesoscale self-assembly and transformation of hybrid nanostructures. *Angew. Chem., Int. Ed.* **2003**, *42*, 2350−2365.
(27) Andreassen, J. P. Formation mechanism and morphology in precipitation of vaterite - nano aggregation or crystal growth? *J. Cryst. Growth* **2005**, *274*, 256−264.
(28) Beck, R.; Andreassen, J. P. Spherulitic growth of calcium carbonate. *Cryst. Growth Des.* **2010**, *10*, 2934−2947.
(29) Kulak, A. N.; Iddon, P.; Li, Y. T.; Armes, S. P.; Colfen, H.; Paris, O.; Wilson, R. M.; Meldrum, F. C. Continuous structural evolution of calcium carbonate particles: A unifying model of copolymer-mediated crystallization. *J. Am. Chem. Soc.* **2007**, *129*, 3729−3736.
(30) Wohlrab, S.; Pinna, N.; Antonietti, M.; Colfen, H. Polymer-induced alignment of DL-alanine nanocrystals to crystalline mesostructures. *Chem.−Eur. J.* **2005**, *11*, 2903−2913.
(31) Freij, S. J.; Godelitsas, A.; Putnis, A. Crystal growth and dissolution processes at the calcite-water interface in the presence of zinc ions. *J. Cryst. Growth* **2005**, *273*, 535−545.
(32) de Leeuw, N. H.; Parker, S. C. Surface structure and morphology of calcium carbonate polymorphs calcite, aragonite, and vaterite: An atomistic approach. *J. Phys. Chem. B* **1998**, *102*, 2914−2922.
(33) Imai, H. Self-Organized Formation of Hierarchical Structures. In *Biomineralization I*; Naka, K., Ed.; Springer: Berlin/Heidelberg. 2007; Vol. *270*, pp 43−72.
(34) Fernandez-Diaz, L.; Putnis, A.; Prieto, M.; Putnis, C. V. The role of magnesium in the crystallization of calcite and aragonite in a porous medium. *J. Sediment. Res.* **1996**, *66*, 482−491.
(35) Sunagawa, I. Characteristics of crystal-growth in nature as seen from the morphology of mineral crystals. *Bull. Mineral.* **1981**, *104*, 81−87.
(36) Zhou, G. T.; Yao, Q. Z.; Ni, J.; Jin, G. Formation of aragonite mesocrystals and implication for biomineralization. *Am. Mineral.* **2009**, *94*, 293−302.
(37) Shi, S. X.; Su, Z. Q.; Wei, H.; Chen, X. N. Fabrication of aragonite rosette superstructure through the weak interaction between nonionic polymers and Ca^{2+}. *J. Appl. Polym. Sci.* **2010**, *117*, 3308−3314.
(38) Ramdohr, P.; Strunz, H. *Klockmann, Lehrbuch der Mineralogie*; Ferdinand Enke Verlag: Stuttgart, 1978.
(39) Bragg, W. L. The structure of aragonite. *Proc. R. Soc. London, Ser. A* **1925**, *76*, 425−451.
(40) Krauss, C.; Chateigner, D.; Gil, O. Fully inorganic electrodeposition of pure aragonite prismatic-like textured layers on titanium Foils. *Cryst. Growth Des.* **2008**, *8*, 4378−4382.
(41) Liu, F. L.; Gao, Y. Y.; Zhao, S. Q.; Shen, Q. A.; Su, Y. L.; Wang, D. J. Biomimetic fabrication of pseudohexagonal aragonite tablets through a temperature-varying approach. *Chem. Commun.* **2010**, *46*, 4607−4609.
(42) Zhou, G.-T.; Yao, Q.-Z.; Fu, S.-Q.; Guan, Y.-B. Controlled crystallization of unstable vaterite with distinct morphologies and their polymorphic transition to stable calcite. *Eur. J. Mineral.* **2008**, *22*, 259−269.
(43) Zhang, Q.; Ren, L.; Sheng, Y.; Ji, Y.; Fu, J. Control of morphologies and polymorphs of $CaCO_3$ via multi-additives system. *Mater. Chem. Phys.* **2010**, *122*, 156−163.
(44) Gehrke, N.; Colfen, H.; Pinna, N.; Antonietti, M.; Nassif, N. Superstructures of calcium carbonate crystals by oriented attachment. *Cryst. Growth Des.* **2005**, *5*, 1317−1319.
(45) Granasy, L.; Pusztai, T.; Tegze, G.; Warren, J. A.; Douglas, J. F. Growth and form of spherulites. *Phys. Rev. E* **2005**, 72.
(46) Burton, W. K.; Cabrera, N.; Frank, F. C. The growth of crystals and the equilibrium structure of their surfaces. *Philos. Trans. R. Soc. London, Ser. A* **1951**, *243*, 299−358.
(47) Pasarín, I. S.; Yang, M.; Bovet, N.; Glyvradal, M.; Nielsen, M. M.; Bohr, J.; Feidenhans'l, R.; Stipp, S. L. S., Molecular ordering of ethanol at the calcite surface. *Langmuir*, accepted, http://pubs.acs.org/doi/pdf/10.1021/la2021758.
(48) Sand, K. K.; Yang, M.; Makovicky, E.; Cooke, D. J.; Hassenkam, T.; Bechgaard, K.; Stipp, S. L. S. Binding of ethanol on calcite: The role of the OH bond and its relevance to biomineralization. *Langmuir* **2010**, *26*, 15239−15247.